IEEE Access
Multidisciplinary | Rapid Review | Open Access Journal

Received 6 September 2022, accepted 16 September 2022, date of publication 21 September 2022,
date of current version 29 September 2022.

Digital Object Identifier 10.1109/ACCESS.2022.3208258

RESEARCH ARTICLE

A Novel PID Controller Cascaded With Higher Order Filter for FOPDT With Real Time Implementation

KURUNA DIVAKAR AND M. PRAVEEN KUMAR
School of Electrical Engineering, Vellore Institute of Technology, Vellore, Tamil Nadu 632014, India
Corresponding author: M. Praveen Kumar (praveen.m@vit.ac.in)

ABSTRACT This work describes the design of Proportional-Integral-Derivative(PID) controller for stable and unstable First Order Processes with Dead Time(FOPDT). PID controller is augmented with a higher order filter. The PID and the filter parameters are analytically derived using polynomial method. Higher order time delay approximation has been considered for improved accuracy. Maximum sensitivity(MS) based analytical tuning procedure is presented and concrete tuning guidelines are derived. The suggested technique is validated against delay dominant and nonlinear processes. In terms of the various performance indices, the suggested technique is compared to existing methodologies. The proposed method is tested on a real time process to verify the practical application.

INDEX TERMS Unstable process, dead time, PID, maximum sensitivity, Pade-2.

I. INTRODUCTION

Industrial process control is crucial and responsible for the quality of the final product, process safety etc. The effective control scheme can lead to significant improvements in various aspects of the process. The most extensively employed and accepted industrial regulator is PID controller. After the tuning guidelines that are proposed by Ziegler *et al.* [1], many researchers have supported to the development of various tuning techniques for various types of processes. In the chemical industry, unstable and integrating processes coexist with stable processes. Designing and tuning a PID controller takes more effort for unstable processes compared to stable processes. For unstable processes, several researchers have suggested ingenious conceptions [2], [3], [4], [5], [6], [7], [8], [9], [10], [11], [12], [13], [14], [15], [16], [17], [18], [19], [20], [21]. When a process associated with dead time (time delay), design and tuning becomes more intricate. Among the reported methods, there exists several multi-loop control techniques with or without smith predictor. Multi loop control structures offers advantage of dealing servo and regulatory responses independently. This feature enables for independent tuning of servo and regulatory responses. But, it is difficult to analyse multi-loop control structures and tuning also becomes cumbersome process.

The goal of this study is to provide a simple and effective control method for unstable and stable FOPDT. A few of the remarkable control strategies that are aimed to control the Unstable First order Process with Dead time (UFOPDT) are shortly covered here. For unstable processes, the Smith predictor in its pristine form is not felicitous. Paor [2] has developed a new variant of smith predictor based control strategy for unstable processes. This modified smith predictor has been amended by several of researchers since then [2], [3], [4], [7], [8], [9], [10], [11], [13], [15], and [16]. In addition to the modified Smith predictor control strategies, several authors [5], [6], and [21] have developed internal model control (IMC) based control techniques. The two degrees of freedom (2 DOF) control structure that has been developed by Ajmeri and Ali [18] can control the set point tracking and disturbance rejection responses independently. However, this approach is acceptable for the diminutive time delay to time constant ratios (θ/τ) only. Furthermore, it utilizes three controllers that leads to intricacy in achieving tuning rules.

The associate editor coordinating the review of this manuscript and approving it for publication was Zhong Wu.

A simple control structure for UFOPDT has been proposed by Begum *et al.* [19]. They have provided detailed tuning guidelines predicated on MS value. However, this technique is not intended for delay dominant processes. Wang *et al.* [21] have proposed an IMC-predicted simple conventional control technique. Although this method is simple in terms of structure and tuning, it performs poorly if the UFOPDT is delay dominant. Muro-Cuellar *et al.* [16] have proposed an observer-based control scheme for UFOPDT.This technique is a modification of the Smith predictor. Multiple controllers and control loops are used in this method, which has an intricate control structure. Moreover, depending on the value of (θ/τ), the control scheme surmises distinct structures. This approach is remarkable for its ability to effectively control delay dominated processes. Tan [15] has presented a control mechanism for UFOPDT. Even for delayed dominant processes, this structure can generate effective control performance. However, this system uses a massive number of controllers and control loops and is difficult to be tuned.

A good control structure is one that is simple in construction, easy to tune, and capable of controlling complex processes like delay dominated processes. The proposed work aims to develop a control method for UFOPDT that is both simple and effective.The highlights of the proposed work are:

- A conventional control structure with a set point filter is employed in the proposed method. To enhance the performance, PID controller is cascaded with a fourth-order filter.
- In order to derive controller parameters, higher order dead time approximation is used to achieve more accuracy.
- Analytically derived tuning rules are proposed with respect to the value of θ/τ.
- The proposed method is successfully verified on a real time process.

The next sections delve more into the current project: The proposed control technique is discussed in Section 2, which also includes the controller architecture, description of set point filter, and tuning parameter. Section 3 comprises of comparison of the proposed method with existing methods. The real-time implementation of the suggested controller is discussed in Section 4, and the conclusion is presented in Section 5.

II. MATHEMATICAL ANALYSIS OF PROPOSED CONTROLLER

The method of deriving PID parameters is not unique. Several researchers have employed model based techniques in deriving PID parameters([5], [6], [14], [19], [20], [21], [22]). Optimization based derivation of PID parameters is also popular among the researchers([23], [24], [25], [26]).The present method has employed a model based technique i.e. polynomial technique to derive the unknown controller parameters. Figure 1 shows the proposed control structure which employs a conventional feedback structure with a set point filter. In Figure 1, r indicates set point, F is set point filter, Gc represents PID controller cascaded with fourth order filter, d is process input disturbance, Gp indicates process and y is process output. To reduce servo response overshoot and alter servo response speed, the set point filter is utilised. The generalised transfer function of UFOPDT is shown in Equation 1.

$$G_p = \frac{ke^{-s\theta}}{(\tau s - 1)} \tag{1}$$

where k, θ,τ represents gain of the process, dead time, process time constant respectively. Equations 2 and Equation 3 represent the servo and regulatory responses respectively.

$$\frac{y}{r} = \frac{FG_C G_p}{(1 + G_c G_P)} \tag{2}$$

$$\frac{y}{d} = \frac{G_p}{(1 + G_c G_p)} \tag{3}$$

A. DESIGN OF CONTROLLER (G_c)

The current study considers a PID controller cascaded with fourth order filter as shown in Equation 4.

$$G_c = \frac{q}{p} = \left(k_p + \frac{k_i}{s} + k_d s\right) \frac{(a_2 s^2 + a_1 s + 1)^2}{(b_2 s^2 + b_1 s + 1)(b_3 s + 1)^2} \tag{4a}$$

$$\text{where,} q = (k_d s^2 + k_p s + k_i)(a_2 s^2 + a_1 s + 1)^2 \tag{4b}$$

$$p = s(b_2 s^2 + b_1 s + 1)(b_3 s + 1)^2 \tag{4c}$$

As illustrated in Equation 5, the process without delay can be expressed as a ratio of two polynomials.

$$G_p = \frac{ke^{-s\theta}}{(\tau s - 1)} = \frac{u}{v} e^{-s\theta} \tag{5a}$$

where,

$$u = k \tag{5b}$$

$$v = \tau s - 1 \tag{5c}$$

Equation 6 and Equation 7, as shown at the bottom of the page, represent servo and regulatory responses respectively which are derived by substituting Equations 4 and 5 into Equations 2 and 3.

When creating a control loop, stability of the closed loop is critical. The roots of characteristic equation (CE) shown

$$\frac{y}{r} = \frac{F(k_d s^2 + k_p s + k_i)(a_2 s^2 + a_1 s + 1)^2 k e^{-s\theta}}{\left(s(b_2 s^2 + b_1 s + 1)(b_3 s + 1)^2(\tau s - 1) + (k_d s^2 + k_p s + k_i)(a_2 s^2 + a_1 s + 1)^2 k e^{-s\theta}\right)} \tag{6}$$

$$\frac{y}{d} = \frac{s(b_2 s^2 + b_1 s + 1)(b_3 s + 1)^2 k e^{-s\theta}}{\left(s(b_2 s^2 + b_1 s + 1)(b_3 s + 1)^2(\tau s - 1) + (k_d s^2 + k_p s + k_i)(a_2 s^2 + a_1 s + 1)^2 k e^{-s\theta}\right)} \tag{7}$$

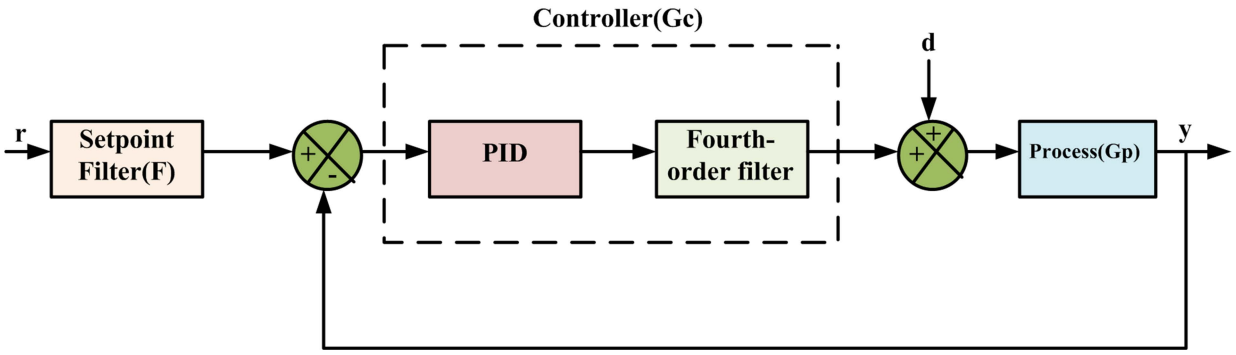

FIGURE 1. Proposed control structure.

in Equation 8 are key to describe the closed loop stability dynamics of the proposed control scheme.

$$s(b_2s^2+b_1s+1)(b_3s+1)^2(\tau s-1) + (k_ds^2+k_ps+k_i)(a_2s^2+a_1s+1)^2ke^{-s\theta}=0 \quad (8)$$

To obtain the unknown controller settings, it is customary to solve the CE in Equation 8 against a desired CE using a dead time approximation. A Taylor's series approximation or a Pade's approximation is used for dead time representation in many studies. Pade's 1^{st} order approximation of dead time is the most often employed method. However, in this study, a higher order approximation i.e. Pade's shift (Pade-2) approximation is considered to obtain more precision. Equation 9 shows the formulation of Pade's shift approximation.

$$e^{-s\theta}=\frac{(1-(s\theta/2n)+\frac{1}{3}(s\theta/2n)^2)^n}{(1+(s\theta/2n)+\frac{1}{3}(s\theta/2n)^2)^n} \quad (9)$$

Equation 9 assumes Pade's second order approximation when n=1. To improve accuracy, the authors have carried investigation considering n = 2.

$$e^{-s\theta}=\frac{(1-(s\theta/4)+(s^2\theta^2/48))^2}{(1+(s\theta/4)+(s^2\theta^2/48))^2} \quad (10)$$

With the assumptions $a_2=\theta^2/48$ and $a_1=\theta/4$, Equation 10 is substituted in Equation 8, resulting a simplified CE as indicated in Equation 11.

$$s(b_2s^2+b_1s+1)(b_3s+1)^2(\tau s-1) + (k_ds^2+k_ps+k_i)k(1-(\theta s/4)+(\theta^2s^2/48))^2=0 \quad (11)$$

Additional simplification leads to the CE as illustrated in Equation 12, as shown at the bottom of the page. The PID values are obtained by solving Equation 12 against a target CE. The authors initial assumption is to have the target CE as illustrated in Equation 13. This choice sets the location of the closed loop poles at $s=-\frac{1}{\lambda}$. However, the authors have identified that this choice does not provide a effective

$$c_6s^6+c_5s^5+c_4s^4+c_3s^3+c_2s^2+c_1s+1=0 \quad (12a)$$

$$c_6=\frac{\tau b_2b_3^2+\frac{kk_d\theta^4}{2304}}{kk_i} \quad (12b)$$

$$c_5=\frac{b_2(-b_3^2+2\tau b_3)-\left(\frac{kk_d\theta^3}{96}\right)+\left(\frac{kk_p\theta^4}{2304}\right)+\tau b_1b_3^2}{kk_i} \quad (12c)$$

$$c_4=\frac{b_1(-b_3^2+2\tau b_3)+\tau b_3^2-b_2(2b_3-\tau)+\left(\frac{5kk_d\theta^2}{48}\right)+\left(\frac{kk_i\theta^4}{2304}\right)-\left(\frac{kk_p\theta^3}{96}\right)}{kk_i} \quad (12d)$$

$$c_3=\frac{2\tau b_3-b_2+b_1(\tau-2b_3)-b_3^2+\left(\frac{5kk_p\theta^2}{48}\right)-\left(\frac{kk_d\theta}{2}\right)-\left(\frac{kk_i\theta^3}{96}\right)}{kk_i} \quad (12e)$$

$$c_2=\frac{\tau-b_1-2b_3+kk_d+\left(\frac{5kk_i\theta^2}{48}\right)-\left(\frac{kk_p\theta}{2}\right)}{kk_i} \quad (12f)$$

$$c_1=\frac{kk_p-\left(\frac{kk_i\theta}{2}\right)-1}{kk_i} \quad (12g)$$

solution, especially for delay-dominated processes.

$$(\lambda s + 1)^6 = 0 \tag{13}$$

As a result, as indicated in Equation 14 and Equation 15, numerous options for desired CE are coined.

$$(\lambda s + 1)^2(a_2 s^2 + a_1 s + 1)^2 = 0 \tag{14}$$

$$(\lambda s + 1)^4(b_3 s + 1)^2 = 0 \tag{15}$$

The idea of having multiple pole locations in the target CE is to reduce the overshoot in response which is caused by the controller-inserted zeroes in the set point tracking or disturbance rejection responses. However, these tests likewise failed to generate a viable system that could provide a stable controller. The authors have, however, arrived at the desired CE polynomial that provides a reliable controller after several attempts. Equation 16 shows the proposed desired CE.

$$(\lambda s + 1)^3(a_2 s^2 + a_1 s + 1)(b_3 s + 1) = 0 \tag{16}$$

The chosen target CE can nullify the effect of few of the zeros in the servo and regulatory responses and locate the other poles at $s = -1/\lambda$.

B. SELECTION OF TUNING PARAMETER(λ)

The suggested technique's tuning rules are determined analytically predicated on maximum sensitivity (MS). Robust stability is measured by MS, and several researchers have successfully proposed tuning criteria using it ([14], [18], [19], [20], [21]). MS is the reciprocal of the shortest distance between the Nyquist curve of the loop transfer function and the critical point. The higher the value of MS, the faster will be the response, but at the expense of stronger stability, and vice versa. As a result, choosing MS involves a trade-off between response time and stability. A unique procedure is followed for both stable and unstable FOPDT. It is identified that, for a particular θ/τ ratio, to achieve a particular MS value, the tuning parameter i.e λ is a function of θ. In other words, for two different processes with the same θ/τ ratio, at a particular MS value, The λ/θ ratios of those two processes are equal [20]. Figure 2 depicts the MS profile for a normalised UFOPDT. From Figure 2, it is observed that the steepness of the plot is relatively less for lower θ/τ values. Because of less steepness, stability of the closed loop system is maintained and less affected by the parameter uncertainty. From figure 2, we can also find the acceptable λ range and corresponding MS profile to alter the robustness. It is also established that as the value of θ/τ rises, the minimal MS that can be achieved rises as well. Table 1 shows the lowest possible minimum MS that can be achieved w.r.t θ/τ. To alter the speed of response, a specific range of tuning parameters is always required. Table 2 shows different tuning ranges based on the θ/τ value. In the case of a θ/τ value larger than 1, it is recommended to keep to λ, which corresponds to the lowest MS.

If the values of k and τ in Equation 5 are negative, the process is FOPDT. Figure 3 shows the effect of the θ/τ ratio on minimum MS values for stable FOPDT. Table 3 shows relation between λ and minimum possible MS value w.r.t θ/τ. Table 4 shows the range of MS and λ values that are possible for the given θ/τ.

TABLE 1. For UFOPDT: Minimum possible MS and corresponding λ.

θ/τ	λ	Minimum possible MS
0.1	3.42θ	1.77
0.2	2.20θ	2.10
0.3	1.57θ	2.43
0.4	1.28θ	2.76
0.5	1.08θ	3.12
0.6	0.93θ	3.50
0.7	0.83θ	3.91
0.8	0.74θ	4.34
0.9	0.75θ	4.84
1	0.85θ	5.56
1.1	0.91θ	6.48
1.2	1.05θ	8.06
1.3	1.22θ	10.5
1.4	1.47θ	14.7
1.5	1.84θ	22.44
1.6	2.48θ	39.54
1.7	3.86θ	92.37
1.8	8.92θ	472.42

TABLE 2. λ range for UFOPDT.

$\frac{\theta}{\tau}$	λ	Corresponding range of MS
0.1	1.29θ to 7.4θ	1.77 to 2
0.2	0.525θ to 6.05θ	2.10 to 3
0.3	0.555θ to 3.55θ	2.43 to 3
0.4	0.7θ to 2.1θ	2.76 to 3
0.5	0.55θ to 2.4θ	3.12 to 4
0.6	0.7θ to 1.65θ	3.5 to 4
0.7	0.66θ to 1.75θ	3.91 to 5
0.8	0.707θ to 1.35θ	4.34 to 5
0.9	0.75θ to 1.355θ	4.84 to 6
1	0.85θ to 1.05θ	5.56 to 6

TABLE 3. For stable FOPDT:Minimum possible MS and corresponding λ.

θ/τ	λ	Minimum possible MS
0.1	20.3θ	1.1681
0.2	10.35θ	1.1819
0.3	7.03θ	1.194
0.4	5.52θ	1.2062
0.5	4.35θ	1.2175
0.6	3.66θ	1.228
0.7	3.28θ	1.238
0.8	2.625θ	1.252
0.9	2.666θ	1.256
1	2.46θ	1.264
1.1	2.273θ	1.272
1.2	2.108θ	1.279
1.3	1.992θ	1.285
1.4	1.892θ	1.292
1.5	1.8133θ	1.297
1.6	1.743θ	1.303
1.7	1.6705θ	1.308
1.8	1.622θ	1.313
1.9	1.684θ	1.333
2	1.71θ	1.330

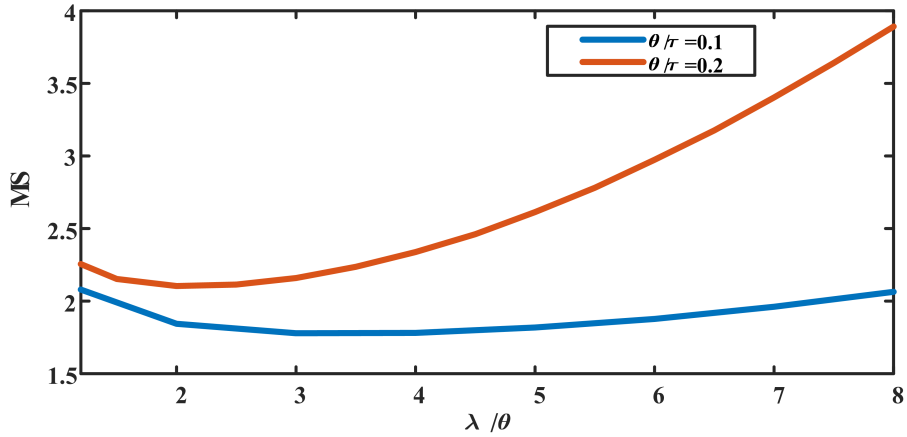

FIGURE 2. Relation between $\frac{\lambda}{\theta}$ and MS.

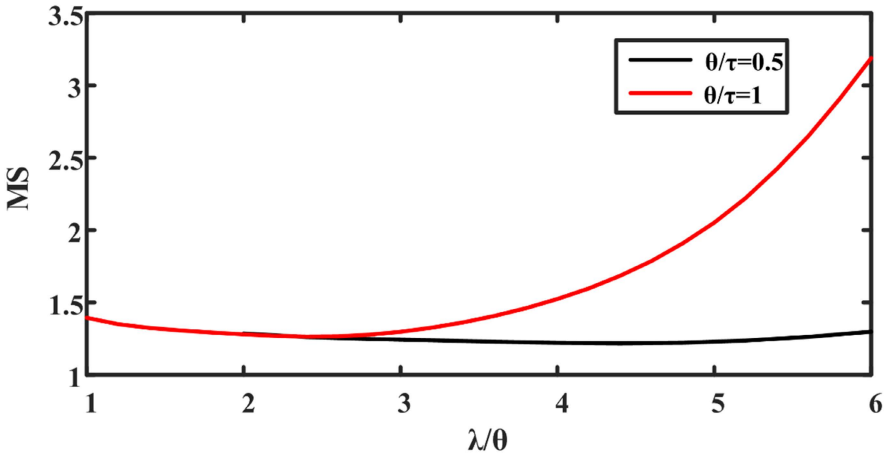

FIGURE 3. Relationship between $\frac{\lambda}{\theta}$ and MS for stable FOPDT.

TABLE 4. λ range for stable FOPDT.

θ/τ	λ	Corresponding range of MS
0.4	3.75θ to 11.25θ	1.475 to 2.22
0.5	1θ to 9θ	1.533 to 2
0.6	2.5θ to 7.5θ	1.259 to 2
0.7	2.143θ to 6.42θ	1.273 to 1.912
0.8	1.875θ to 5.87θ	1.288 to 2
0.9	1.667θ to 5.44θ	1.302 to 2
1	1.5θ to 5θ	1.315 to 2
1.5	1θ to 3.733θ	1.379 to 2
2	0.75θ to 3.25θ	1.435 to 2

C. SET POINT FILTER

Researchers commonly employ a setpoint filter to alter the servo response. The controller introduced zeros may cause overshoot in the servo response. A set point filter, as shown in Equation 17, is proposed to suppress the overshoot in servo response.

$$F = \frac{\gamma s + 1}{\left(\frac{k_d}{k_i}s^2 + \frac{k_p}{k_i}s + 1\right)(a_2 s^2 + a_1 s + 1)} \tag{17}$$

The suggested filter suppresses the effect of zeros introduced by the controller, and the servo response speed can be adjusted using the newly introduced tuning parameter γ. However, because it is outside the closed loop, this tuning parameter has no effect on the stability of the closed loop system. As a result, when it comes to the closed loop stability, γ selection is a trivial process.

III. SIMULATION ANALYSIS

In this section, various subsisting control strategies are considered and compared to the suggested solution. Equations 18-21 provide a mathematical representation of a variety of widely used assessment parameters.

$$Integral\ Absolute\ Error(IAE) = \int_0^\infty |e(\tau)|d\tau \tag{18}$$

$$Integral\ Square\ Error(ISE) = \int_0^\infty e^2(\tau)d\tau \tag{19}$$

$$Integral\ Time\ Absolute\ Error(ITAE) = \int_0^\infty \tau|e(\tau)|d\tau \tag{20}$$

TABLE 5. Controller settings of other methods.

Process	Method	Controller parameters
$\frac{1}{(s-1)}e^{-0.5s}$	G.Lloyds et.al [27]	$k_c = 0.4377, T_i = 1.1725,$ $k_p = 1.560, T_d = 0.25$
$\frac{1}{(s-1)}e^{-1.2s}$	Tan W [15]	$K_o = 2, K_1 = \frac{s+1}{2s+1},$ $K_2 = \frac{0.02821s^3+0.1828s^2+0.7374s+1.135}{0.00552s^3+0.0511s^2+0.04532s+1},$ $K_3 = \frac{s+1}{2s+1}$
	Kumar.et.al [20]	$k_p = 1.1343, k_i = 0.0198, k_d = 0.4519$ $a_1 = 0.6, a_2 = 0.12, \lambda_s = 0.5$ $f_R = \frac{5.922s^4+15.85s^3+14.60s^2+6.24s+1}{0.17s^8+222.5s^7+17.9s^6+68.605s^5+158.8s^4+222.5s^3+174.5s^2+59.8s+1}$
$\frac{6}{(s-1)}e^{-1.5s}$	Del Muro-Cuellar.et.al [16]	$K = 0.4841, T_i = 3.2021, \sigma = 0.35$ $g_1 = 0.6, g_2 = 0.27, g_3 = 1.6$
Nonlinear process	Ajmeri and Ali [18]	$\alpha = 10, \beta = 5.1556, k_c = 2.5437, K_{p1} = 0.3754$ $T_{i1} = 10, K_{p2} = 1.0665,$ $T_{i2} = 121.0663$
$\frac{1}{(s+1)}e^{-2s}$	Vijayan et.al [17]	$K_p = 0.3147, K_i = 0.7983, K_d = 0.539$ $T_f = \frac{1}{0.9s+1}$
Quanser DC servo motor	zhao et.al [22]	$K_p = 0.00707, K_i = 0.0414.$

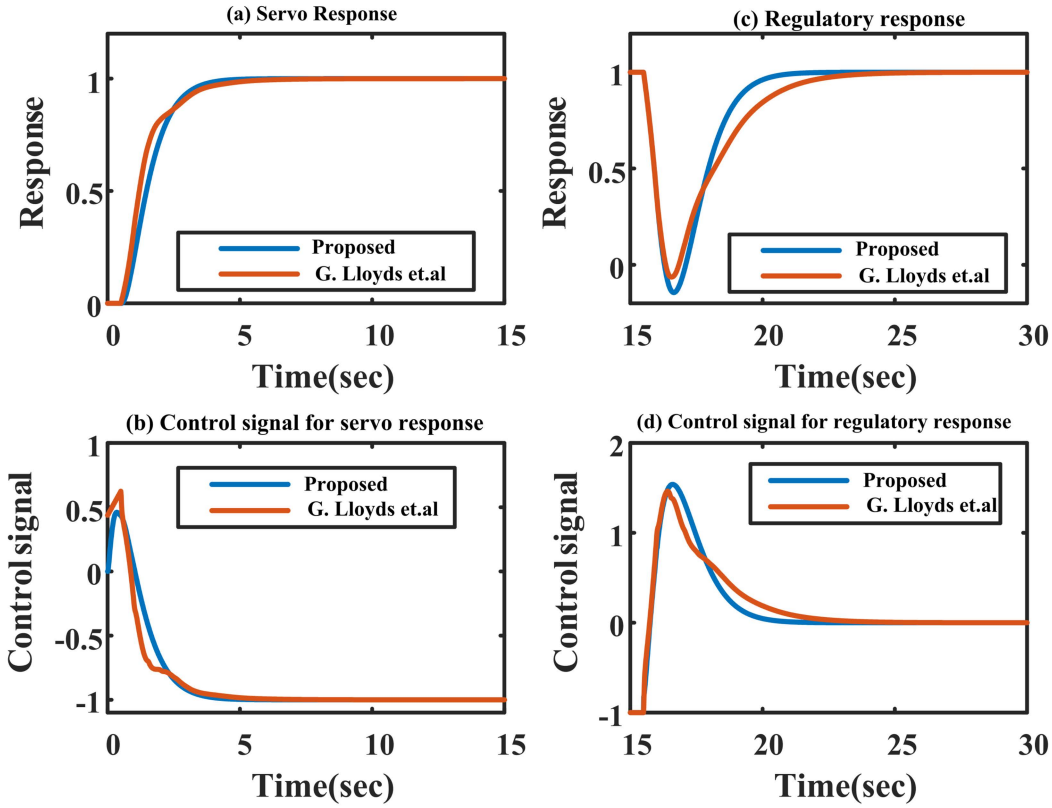

FIGURE 4. Responses for Example 1 under no model mismatch condition.

$$Total\ Variation(TV) = \sum_{j=0}^{\infty} |u_{j+1} - u_j| \quad (21)$$

where u_j represents the controller input to the process at j^{th} instant, and e denotes error. Control loops that are tuned for IAE respond with fewer oscillations. Large errors are yarely eliminated by control loops that are tuned for ISE. ITAE-optimized control loops result in more expeditious settling times relatively. To safeguard the final control element from wear and tear, it's critical to ensure smooth fluctuations in the input to the process. TV is an estimation of the smoothness of the process input that should be taken into account. In order to calculate TV, the process input is sampled at 0.1s intervals.

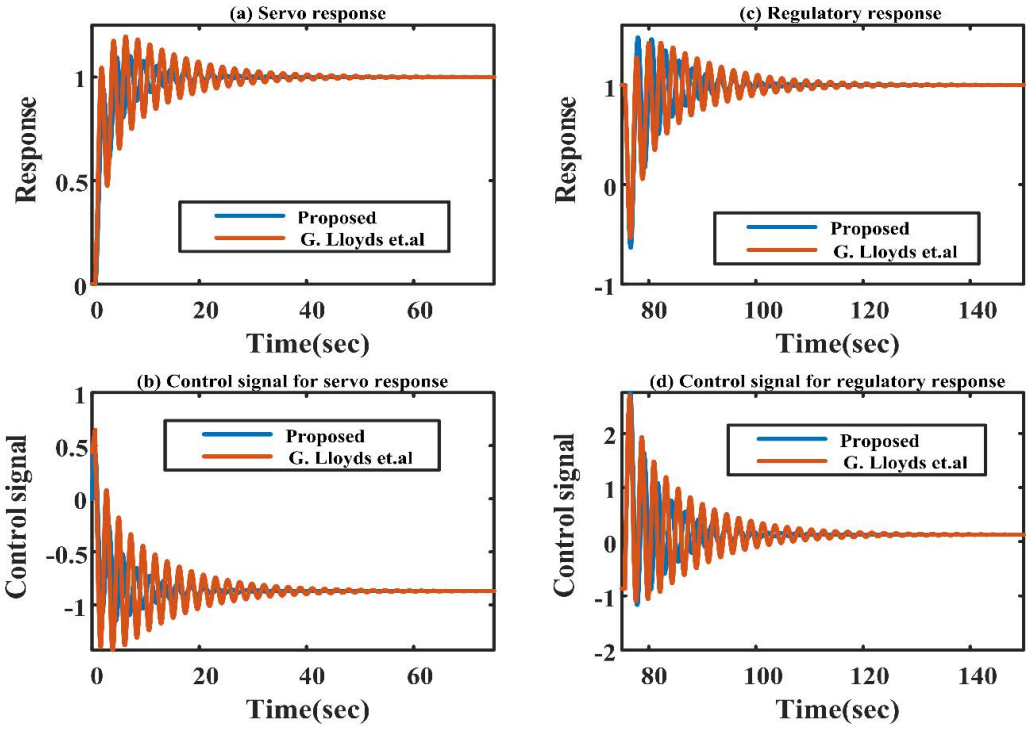

FIGURE 5. Responses for Example 1 under model mismatch condition.

TABLE 6. Controller Settings of the proposed method.

Example	Process	k_p	k_i	k_d	PID Filter	λ	γ
1	$\frac{1}{(s-1)}e^{-0.5s}$	1.8663	0.4287	0.0481	$\frac{(0.0052s^2+0.125s+1)^2}{(0.0116s^2+0.0574s+1)(0.026s+1)^2}$	0.54	0.5
2	$\frac{1}{(s-1)}e^{-1.2s}$	1.2035	0.0432	0.0329	$\frac{(0.03s^2+0.3s+1)^2}{(0.0552s^2+0.0014s+1)(0.0274s+1)^2}$	1.26	2
3	$\frac{6}{(s-1)}e^{-1.5s}$	0.1767	0.0011	0.0071	$\frac{(0.047s^2+0.375s+1)^2}{(0.0982s^2+0.0000773s+1)(0.0402s+1)^2}$	2.75	4
4	Nonlinear process	1.1483	0.0108	1.443	$\frac{(8.333s^2+0.5s+1)^2}{(19.7816s^2+3.3211s+1)(1.2718s+1)^2}$	21	15
5	$\frac{1}{(s+1)}e^{-2s}$	0.2507	0.201	0.0449	$\frac{(0.0833s^2+0.5s+1)^2}{(0.2542s^2+0.7336s+1)(0.2169s+1)^2}$	1.5	0.5
6	Quanser DC servo motor	0.01	0.0502	0.000238	$\frac{(0.0052s^2+0.1250s+1)^2}{(0.0097s^2+0.0711s+1)(0.0278s+1)^2}$	0.2	-

$$f_R : Setpoint filter$$

$$1.f_R = \frac{0.5s+1}{0.0006s^4+0.0367s^3+0.6618s^2+4.478s+1} \quad 2.f_R = \frac{2s+1}{0.0229s^4+1.0637s^3+9.1430s^2+28.1366s+1}$$

$$3.f_R = \frac{4s+1}{0.3101s^4+10.222s^3+68.5919s^2+165.51s+1} \quad 4.f_R = \frac{15s+1}{1113.38s^4+952.8s^3+195.106s^2+106.82s+1}$$

$$5.f_R = \frac{0.5s+1}{0.0186s^4+0.2154s^3+0.9295s^2+1.7460s+1}$$

Example 1:

In this example, the UFOPDT indicated in Equation 22 is taken into consideration for evaluation. Raja and Ali [27], V.Vijayan *et al.* [17], Ajmeri and Ali [18] have analysed this process previously and Raja and Ali method [27] is proved to be superior than the other methods.

$$G_P = \frac{1}{s-1}e^{-0.5s} \tag{22}$$

Table 5 shows the controller parameters for the method of Raja and Ali [27]. In the proposed approach, $\gamma = 0.5$ and

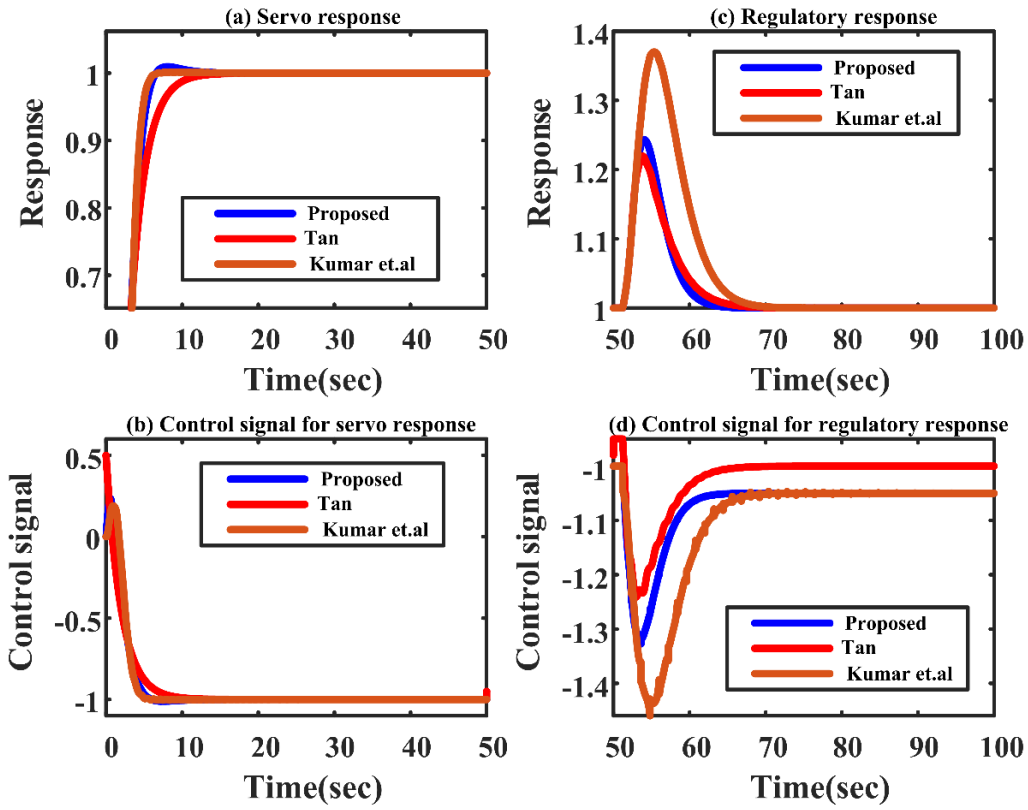

FIGURE 6. Responses for Example 2 under no model mismatch condition.

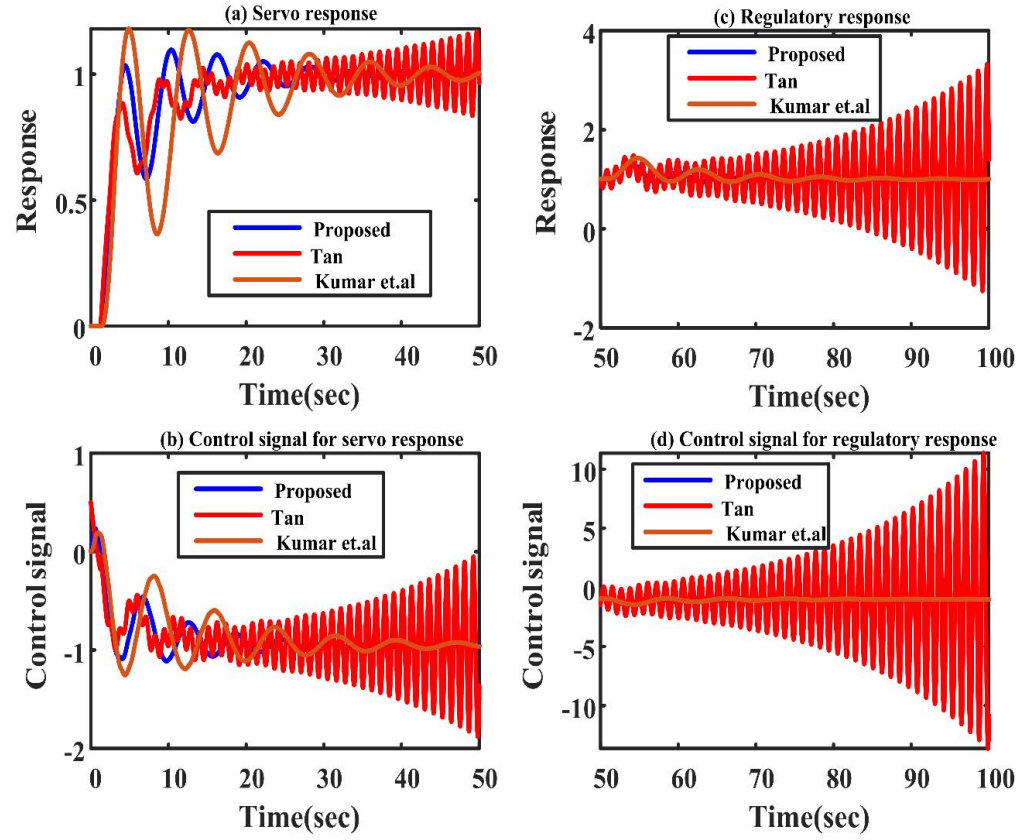

FIGURE 7. Responses for Example 2 under model mismatch condition.

TABLE 8. Comparison matrix under model mismatch condition.

Perturbed process	Method	Servo						Regulatory					
		TV	t_s	IAE	ISE	t_r	OS(%)	TV	t_s	IAE	ISE	t_r	OS(%)
$\frac{1.15e^{-0.575s}}{(0.9s-1)}$	Proposed	7.53	18.72	2.068	1.329	0.97	10.29	25.19	23.57	5.36	3.47	0.384	-56.5
	G.Lloyds et.al [27]	19.43	34.59	3.8	1.432	0.7304	9.37	42	38.95	7.09	3.65	0.3148	-57.68
$\frac{1.05e^{-1.26s}}{(0.95s-1)}$	Proposed	4.51	31.76	5.092	2.755	1.854	3.13	2.21	37.34	1.744	0.251	1.049	24.83
	Kumar et.al [20]	6.154	48.39	8.05	3.98	1.606	18.45	4.738	48.18	3.227	0.6921	2.192	48.12
	Tan W [15]	Unstable						Unstable					
$\frac{6.1e^{-1.5375s}}{(0.975s-1)}$	Proposed	0.262	37.3	7.98	4.44	14.47	0.462	0.147	42.32	2.725	0.472	3.022	1.995
	Del Muro-Cuellar et.al [16]	1.14	50.91	7.764	3.332	1.507	20.98	0.266	53.43	2.94	0.4621	2.892	28.84
Non linear Process	Proposed	5.92	605	649	1322	347.8	0	3.3	303.5	34	5.164	809	4.6
	Ajmeri and Ali [18]	6.93	662	635	1214	349.3	0	3.3	362	41.6	6.4	857	4.7
$\frac{1.1}{(0.9s+1)}e^{-2.2s}$	Proposed	0.993	8.29	4.39	3.72	2.985	17.05	1.059	10.8	1.80	0.65	2.783	-18.45
	Vijayan et.al [17]	3.091	25.81	4.59	3.188	2.50	9.34	4.16	40.4	3.447	0.76	0.596	-146.16

$t_s - Settling\ Time\ (sec)\ \ t_r - Rise\ time\ (sec)\ \ OS - Overshoot(+ : Overshoot, - : Undershoot)$

TABLE 7. Comparison matrix under no model mismatch condition.

Process	Method	Servo						Regulatory					
		TV	t_s	IAE	ISE	t_r	OS(%)	TV	t_s	IAE	ISE	t_r	OS(%)
$\frac{e^{-0.5s}}{(s-1)}$	Proposed	1.92	3.787	1.64	1.22	1.846	0.505	5.07	5.37	2.33	1.84	2.132	-0.505
	G.Lloyds et.al [27]	2.24	4.577	1.5	1.033	2.111	0.49	4.92	7.79	2.67	1.75	3.574	-0.504
$\frac{e^{-1.2s}}{(s-1)}$	Proposed	1.49	5.824	3.08	2.42	2.93	0.505	0.74	12.7	1.15	0.1936	1.697	2.03
	Kumar et.al [20]	1.486	5.66	3.164	2.635	2.33	0.505	1.425	17.24	2.52	0.651	2.42	3.73
	Tan W [15]	2	9.02	3.2	2.2	4.307	0.505	0.59	15.78	1.18	0.169	1.546	1.998
$\frac{6e^{-1.5s}}{(s-1)}$	Proposed	0.193	11.59	5.73	4.22	6.47	1.531	0.1	24.7	2.72	0.522	3.293	1.992
	Del Muro-Cuellar et.al [16]	0.505	5.31	2.48	1.99	2.107	0.502	0.13	34.4	2.40	0.38	3.003	3.890
Nonlinear Process	Proposed	146	584.7	1150	6.53	316.6	0	572	33.92	7.58	4.33	681	3.8
	Ajmeri and Ali [18]	175	602.8	1047	6.76	295.2	0	658	41.63	9.64	4.33	767	4.2
$\frac{1}{(s+1)}e^{-2s}$	Proposed	1	9.03	4.62	3.73	3.557	8.152	1.005	11.16	1.75	0.533	3.314	-9.34
	Vijayan et.al [17]	1.91	10.22	3.87	3.12	3.0785	1.531	2.163	17.62	1.58	0.37	1.454	-36.30

$t_s - Settling\ Time\ (sec)\ \ t_r - Rise\ time\ (sec)\ \ OS - Overshoot(+ : Overshoot, - : Undershoot)$

$\lambda = 0.54$ are considered. Table 6 shows the calculated controller parameters. A step input of magnitude 1 is coerced at $t = 0$ *sec* and a perturbance of negative unit step is imposed at $t = 15$ *sec*. The suggested method performs marginally superior in case of settling time and TV in nominal servo response as shown in Figure 4 and the assessment reported in Table 7. In the case of regulatory response, the suggested method produces superior performance in IAE and settling time.

A $+15\%$ variation in k and θ and -10% variation in τ are coerced to verify the robust stability of the methods. For analysing the regulatory response, a negative unit disturbance is applied at $t = 75$ *sec*. The overall preponderance of the proposed strategy is evident from the response presented in Figure 5 and the comparison matrix shown in Table 8.

Example 2:

This example considers the delay dominant UFOPDT shown in Equation 23.

$$G_p(s) = \frac{1}{s-1}e^{-1.2s} \tag{23}$$

The proposed method is compared with the method proposed by Kumar *et al.* [20] and Tan [15] method. The method of Kumar *et al.* [20] has already been shown to be better than the methods proposed by Tan [15] and Tan *et al.* [6]. Kumar *et al.* [20] and Tan [15] suggested controllers settings are shown in Table 5. The suggested technique is implemented for $\lambda = 1.26$ and $\gamma = 2$ based on the data presented in Table 1 and discussion in Section 2.2. The obtained controller settings are listed in Table 6. For analysing the no model mismatch response, a unit step set point variation is coerced at $t = 0$ sec and a disturbance of 0.05 units is considered at $t = 50$ sec. Figure 6 depicts the perfect model response, while Table 7 depicts the performance analysis. In the overall comparison, it is clear that all strategies performed equally well in servo response. In regulatory condition, Proposed method and Tan [15] method gave superior performance compared to Kumar *et al.* [20] method. The proposed and Kumar *et al.* [20] methods have utilized a basic conventional control structure, whereas the Tan [15] method applied multiple controllers.

A perturbed (model mismatch) performance study is carried out for a $+5\%$ variation in k, a -5% variation in τ, and a $+5\%$ variation in θ. Tan [15]'s approach is incapable of producing stable output, whereas the other methods despite having a simple control structure, are capable of producing stable output. Figure 7 depicts the graphical response, while Table 8 represents the detailed evaluation. It is evident that, the proposed method outperforms the other methods in terms of all the performance indices.

Example 3:

In this example, the delay dominant UFOPDT represented in Equation 24 is analysed.

$$G_p(s) = \frac{6}{s-1}e^{-1.5s} \tag{24}$$

The above process is previously studied by Muro-Cuellar *et al.* [16] and Rao *et al.* [13]. Del Muro-Cuellar *et.al* [16] method proved to be superior than other method. Table 5 shows the controller and its parameters for this method. The controller parameters are calculated using the proposed approach at $\lambda = 2.75$ and $\gamma = 4$. Table 6 shows the resulting controller settings. Figure 8 depicts the nominal response for a unit step as a set point at $t = 0$ *sec* and a perturbance of 0.003 units at $t = 80$ *sec*. In the case of servo response, it can be concluded from the response and analysis shown in Table 7 that the other technique performs superior than the proposed. However, in the instance of regulatory action, the suggested method is capable of producing similar performance.

To examine the robust performance, $+2.5\%$ variation in θ, -2.5% variation in τ and $+1.67\%$ variation in k are used. By observing the response shown in Figure 9 and performance comparison presented in Table 8, it is clear that the proposed method performs better than the other technique. The opposite control method is delivering relatively high oscillations, settling times and large overshoot.

Example 4:

Control strategies developed for linear processes should be applied to a higher order or nonlinear processes in practicality. Nonlinear processes are linearized at an operational point in order to obtain a linear model. The present study considers a previously studied isothermal reactor [11], [18], [19]. Cholette's model describing an isothermal chemical reactor with non-ideal mixing [28] is shown in Equation 25.

$$\frac{dC_A}{dt} = \frac{F}{V}(C_{A0} - C_A) - \frac{k_1 C_A}{(k_2 C_A + 1)^2} \tag{25}$$

where, C_{A0},C_A represents input, output concentrations respectively. V is reactor volume and F is input flow rate. The different operating parameters considered previously by several authors [11], [20], and [18] are $k_1 = 10\ l/sec$, $k_2 = 10\ l/mol$, $V = 1\ l$. This model is investigated at an operating point $F = 0.0333\ l/sec$, $C_{A0} = 3.288\ mol/l$, $C_A = 1.316\ mol/l$. The measurement lag caused by the concentration transducer is assumed to be the source of a dead period of 20 seconds. The linearized model considered by [11], [20], and [18] is shown in Equation 26.

$$\frac{C_A(s)}{C_{A0}(s)} = G_p(s) = \frac{3.433e^{-20s}}{103.1s - 1} \tag{26}$$

According to the data in Table 1, the value of λ is adjusted to 21 (θ/τ is nearer to 0.2), and the value of γ is tuned to 15. Tables 5 and 6 show the controller parameter settings for the methods of Ajmeri and Ali [18] and the proposed method, respectively. At $t = 0$ *sec*, the set point is varied from 1.316 mol/l to 5 mol/l. Disturbance is assumed to be a change in F, which is changed from 0.0333 l/sec to 0.4 l/sec at $t = 2000$ *sec*. Figure 10 depicts the simulation results related to nominal conditions.

Robust performance is examined by taking into account a $+30\%$ variation in measurement lag, a -25% variation in k_1 and a $+25\%$ variation in k_2. Figure 11 depicts the perturbed response. The suggested method has an overall

superior performance, especially in case of disturbance rejection which is evident from the performance indices shown in Tables 7 and 8.

Example 5:

In this example, delay dominant FOPDT is considered (Equation 27).

$$G_p(s) = \frac{1}{s+1}e^{-2s} \tag{27}$$

Vijayan *et al.* [17], Zhang [12] have previously investigated the above process and the method of Vijayan *et al.* [17] has shown superior performance than other method. Vijayan *et al.* [17] method's controller parameter settings are shown in Table 5. The proposed method's controller parameters are obtained at λ is equal to 1.5 and γ is assumed to be 0.5. Table 6 shows the controller parameters of the proposed method. For the simulation study, a unit step input is applied at $t = 0$ *sec* to analyse servo response and a negative disturbance of magnitude 0.5 is applied at $t = 50$ *sec* to analyse the regulatory response. Figure 12 illustrates the nominal response.Table 7 shows a performance comparison between two controllers. According to the responses, the proposed method has less total variance (TV) in servo and regulatory conditions. The process with parametric uncertainty is considered when examining the robust performance. The parametric uncertainties are represented as a $+10\%$ change in k and θ, and a -10% variation in τ. Figure 13 depicts the perturbed condition's response and Table 8 depicts the performance analysis of two control strategies. Table 8 shows that, under the perturbed condition, the proposed method outperforms the opposite method.

IV. REAL TIME IMPLEMENTATION

DC servo motors are widely used in industries for position and speed control applications. The proposed controller's performance in a real-time scenario is evaluated using a Quanser DC servo motor test bench process (Figure.14). The motor is interfaced to the programming environments MATLAB and Simulink through data acquisition system (DAQ). The schematic diagram of Quanser Qube servo process is shown in Figure 15 and mechanical and electrical parameters are presented in Table 9. Equation 28 represents the estimation of the transfer function between voltage and speed using input and output data.

$$G_p(s) = \frac{24.7523}{0.1708s+1} \tag{28}$$

However, in order to validate the proposed method, a time delay is also included. The output is fed back to the controller after being passed through time delay. Equation 29 represents the resultant open loop transfer function.

$$G_p(s) = \frac{24.7523}{0.1708s+1}e^{-0.5s} \tag{29}$$

In a real-time scenario, the proposed method is compared with Zhao *et al.* [22] method. Table 6 lists the tuning parameters of the suggested method obtained at $\lambda = 0.2$. The controller settings of Zhao *et al.* [22] method are presented in Table 5. For a fair comparison, both methods are tuned at the same MS value of 1.6068. A set point of 50 rad/sec is applied at $t = 0$ *sec* and a unit negative magnitude is applied at $t = 25$ *sec*. The response under nominal condition is depicted in Figure 16 and performance matrix is represented in Table 10. From Table 10, it is clear that the proposed method performs better in terms of all performance indices both in servo and regulatory conditions. In servo response, the proposed method performs marginally better in terms of rise time but significantly better in terms of all other performance indices. In regulatory response, the proposed method performs marginally better in terms of rise time and overshoot, but significantly better in terms of all other performance indices.

TABLE 9. Parameters of Qube Servo process.

Parameter	Symbol	Value
DC servo Motor		
Terminal Resistance	R_m	$8.4\,\Omega$
Back emf constant of the motor	K_m	0.042 V/(rad/s)
Rotor Inductance	L_m	1.16mH
Torque Constant	k_t	0.042N.m/A
Rotor Inertia	J_m	$4.0 \times 10^{-6} kgm^2$
Load disk		
Radius of load disk	r_d	0.0248m
Moment of inertia of load disk	J_d	-
Mass of load disk	m_d	0.053 kg
Moment of inertia of hub	J_h	-

In order to analyse the robustness of the proposed controller, a $+20\%$ perturbation is considered in θ. The performance curves of both methods are presented in Figure 17. The comparative analysis of both methods are presented in Table 10. The proposed method outperforms the other method in perturbed conditions also which is evident from Table 10. In servo response, the proposed method performs marginally better in terms of rise time but significantly better in terms of all other performance indices. In regulatory response, the proposed method performs marginally better in terms of rise time and overshoot, but significantly better in terms of all other performance indices.

In order to analyze the set point tracking capabilities of the proposed method, a time-varying set point profile is used. The set point value and the corresponding time at which it is enforced are presented in Equation 30.

$$Set\ point = \begin{cases} 20\ rad/sec, & t = 0\ \ sec \\ 40\ rad/sec, & t = 10\ \ sec \\ 30\ rad/sec, & t = 20\ \ sec \\ 15\ rad/sec, & t = 30\ \ sec \\ 20\ rad/sec, & t = 40\ \ sec \end{cases} \tag{30}$$

The response of time varying set point profile is shown in Figure 18. From the performance curves in Figure 18, it is observed that the suggested control technique not only tracking setpoint changes but also provided a better response compared to the method of Zhao *et al.* [22].

In order to assess the disturbance rejection performance, multiple input disturbances are considered at different

TABLE 10. Performance measures of response of Quanser DC Servo motor.

		Nominal condition											
		Servo						Regulatory					
Process	Method	IAE	ISE	TV	t_r	O.S(%)	t_s	IAE	ISE	TV	t_r	O.S(%)	t_s
$\frac{24.7523e^{-0.5s}}{0.1708s+1}$	Proposed	90.84	2612	3.41	0.909	25.94	9.76	24.95	273.9	1.645	1.288	-1.900	6.4
	Zhao et.al [22]	115.2	3306	4.515	1.07	30.92	11.6	32.34	380.3	2.34	1.349	-1.905	7.25
		Perturbed condition											
		Servo						Regulatory					
Process	Method	IAE	ISE	TV	t_r	O.S(%)	t_s	IAE	ISE	T.V	t_r	O.S(%)	t_s
$\frac{24.7523e^{-0.6s}}{0.1708s+1}$	Proposed	109	3054	3.92	0.866	36.30	13.16	28.8	318.4	1.723	1.127	-1.725	6.97
	Zhao et.al [22]	136.9	3820	5.45	1.037	40.14	15.53	36.88	431.9	2.535	1.252	-1.903	7.49

$t_r - Rise\ time\ (sec)\quad t_s - Settling\ Time\ (sec)\quad OS - Overshoot(+: Overshoot, -: Undershoot)$

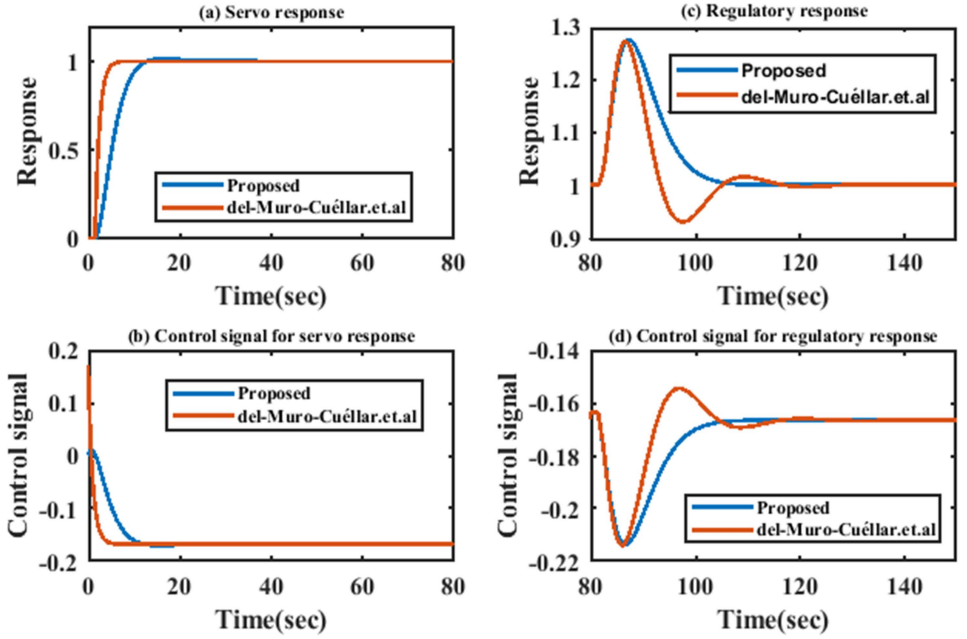

FIGURE 8. Responses for Example 3 under no model mismatch condition.

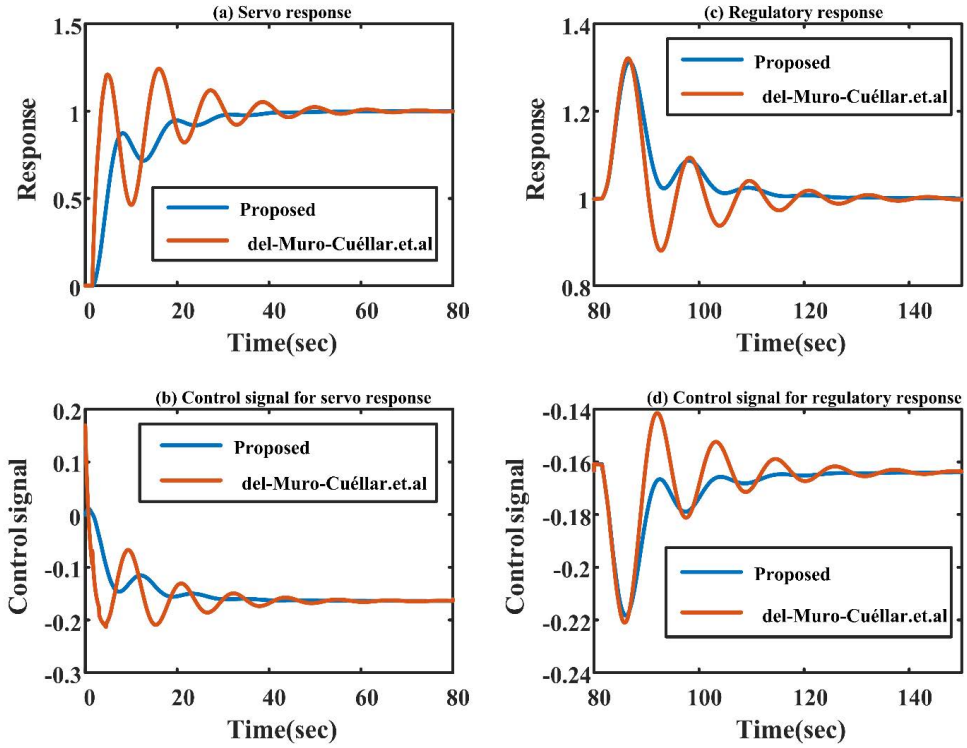

FIGURE 9. Responses for Example 3 under model mismatch condition.

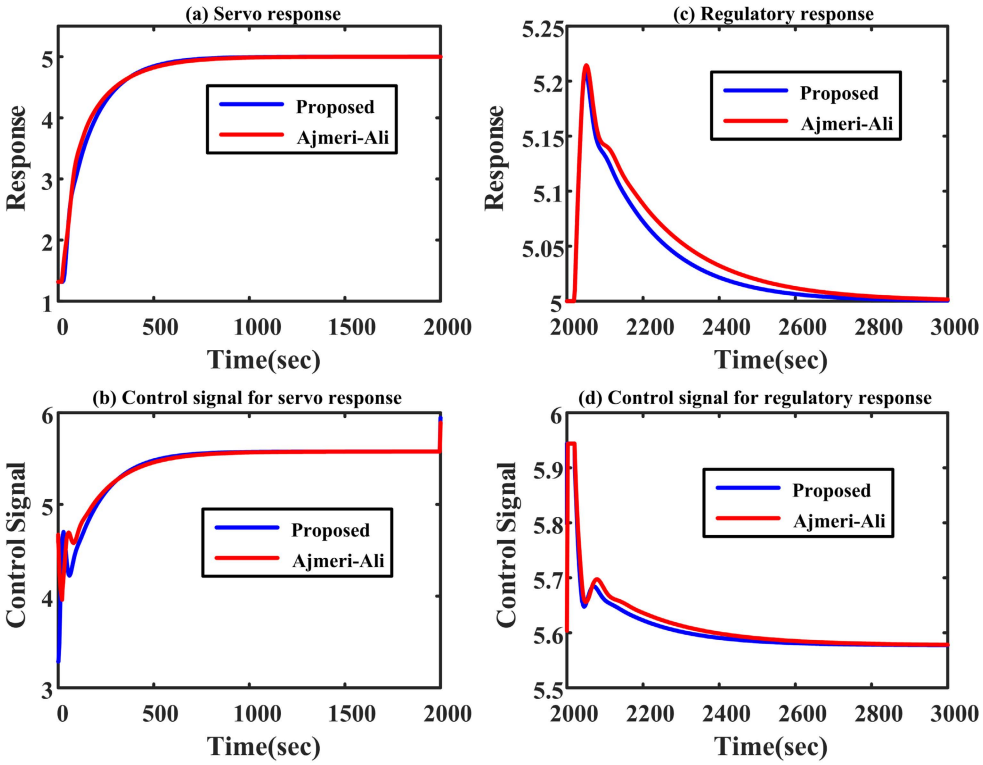

FIGURE 10. Responses for Example 4 under no model mismatch condition.

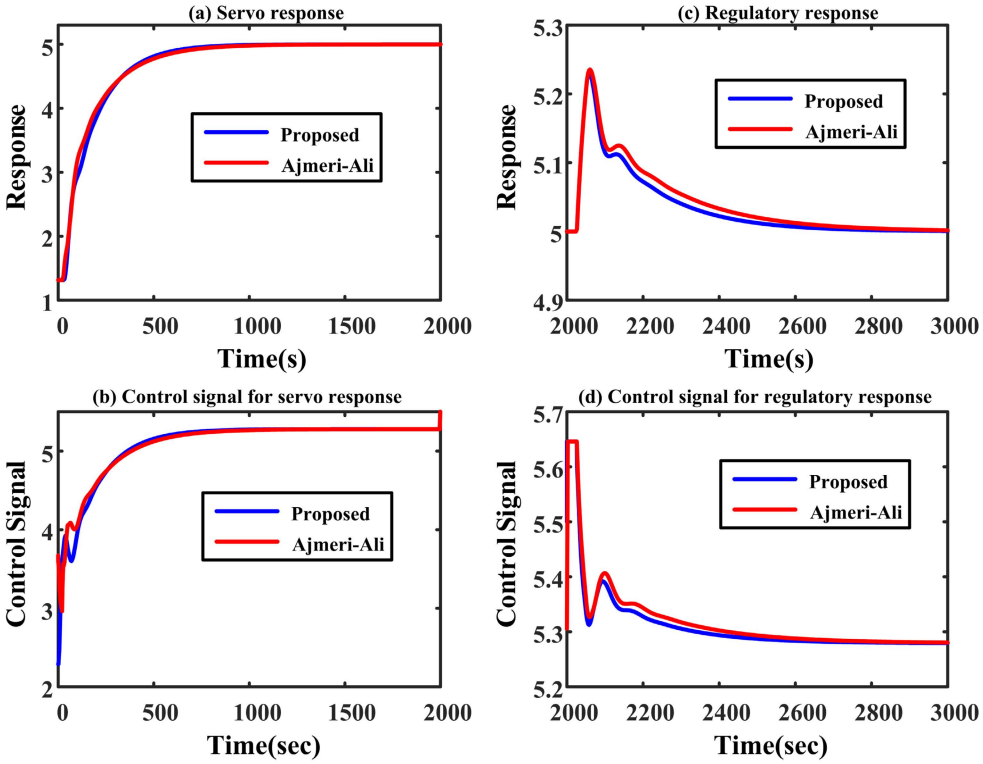

FIGURE 11. Responses for Example 4 under model mismatch condition.

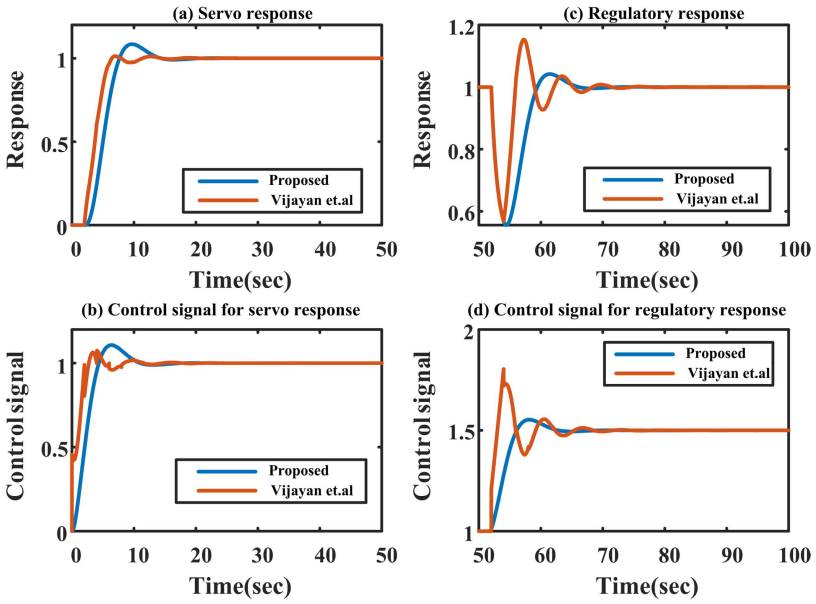

FIGURE 12. Responses for Example 5 under no model mismatch condition.

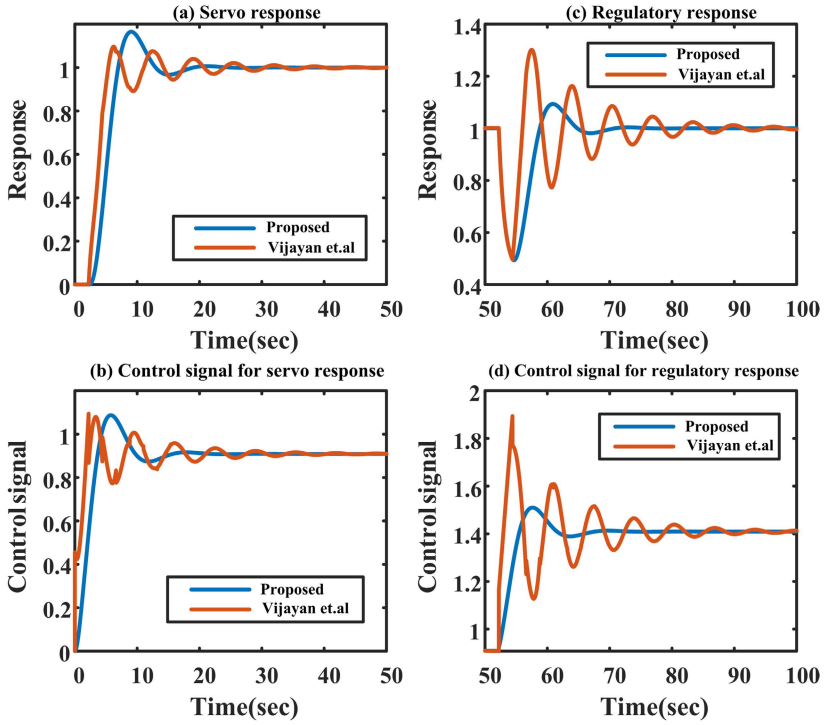

FIGURE 13. Responses for Example 5 under model mismatch condition.

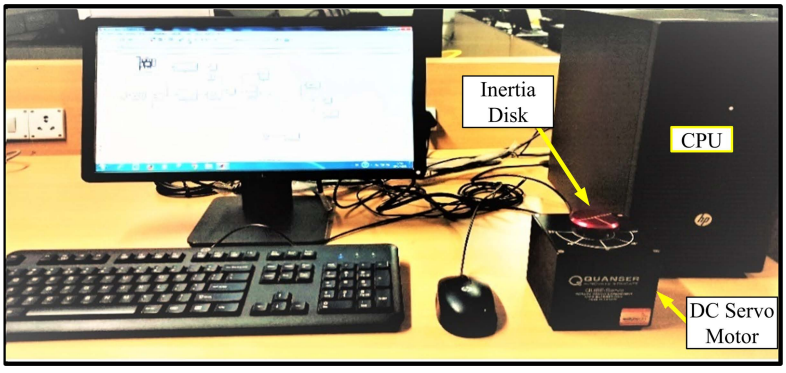

FIGURE 14. Quanser Qube servo plant.

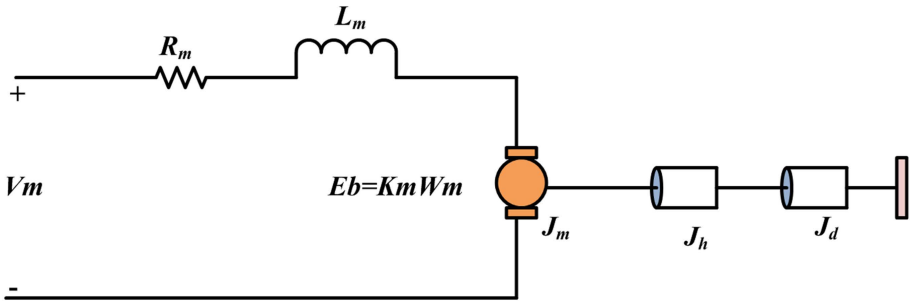

FIGURE 15. Simplified diagram of Qube servo motor.

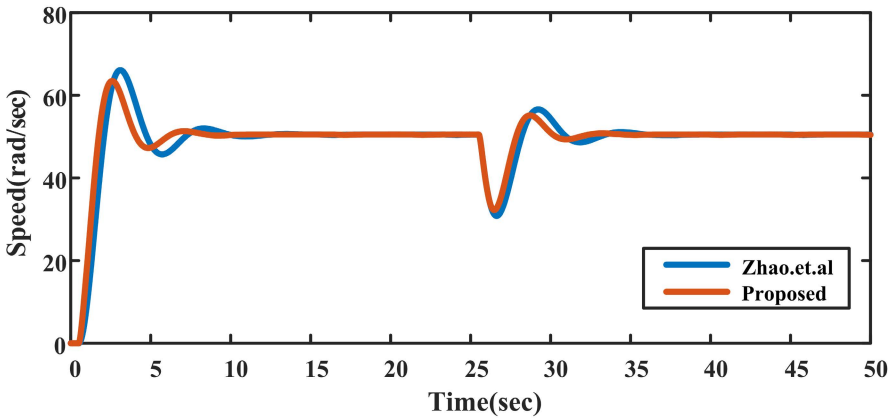

FIGURE 16. Speed response of Quanser DC servo motor under nominal condition.

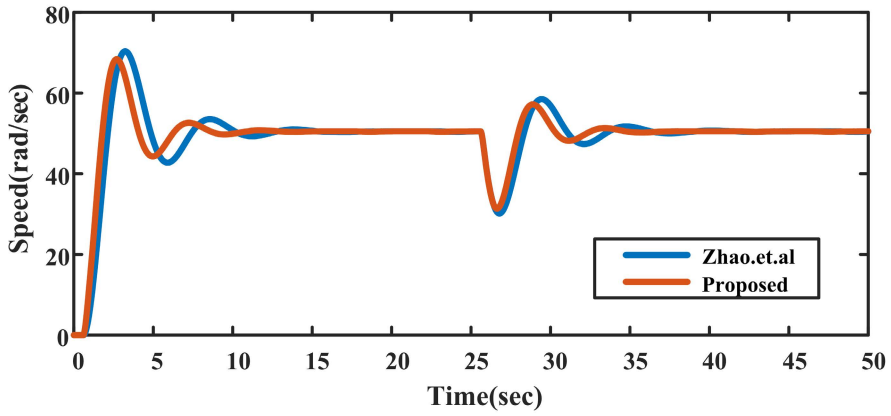

FIGURE 17. Speed response of Quanser DC Servo motor under perturbed condition.

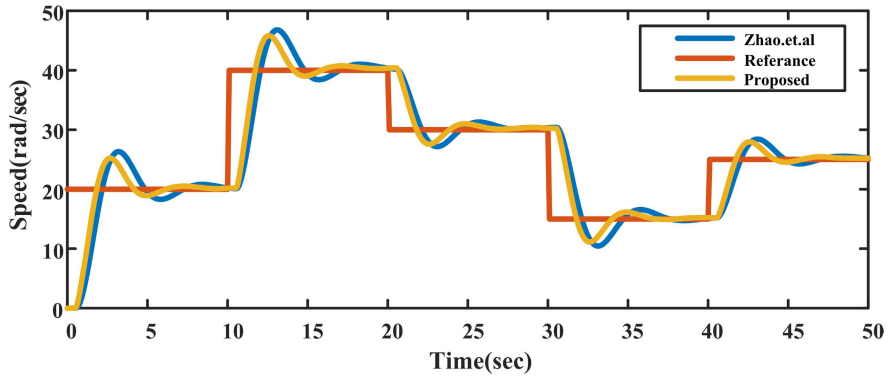

FIGURE 18. Setpoint tracking trajectory of Quanser DC Servo motor.

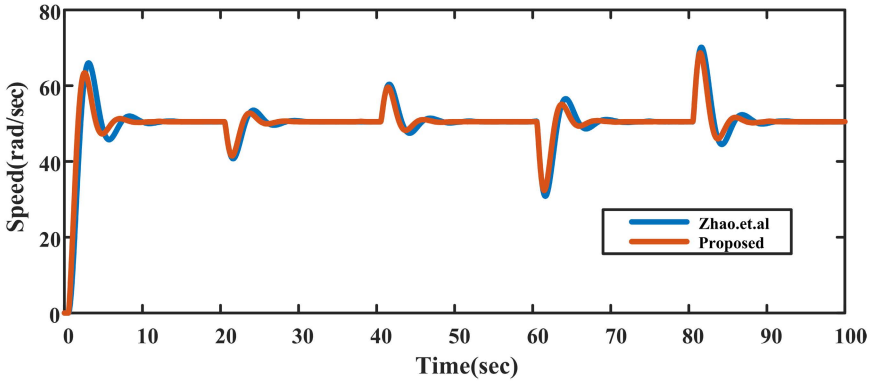

FIGURE 19. Disturbance rejection response of Quanser DC servo motor.

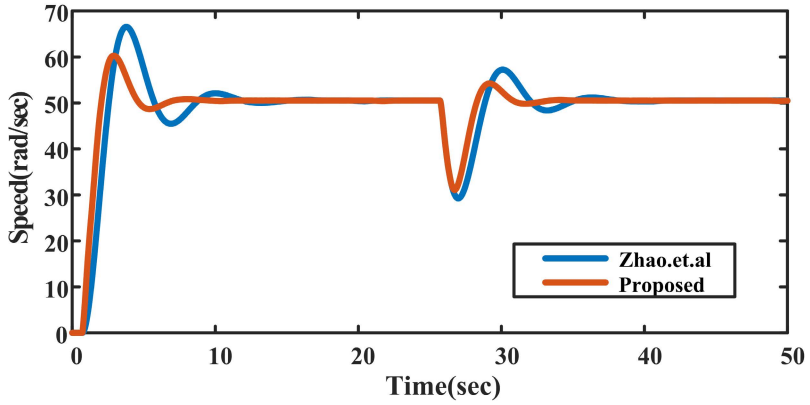

(a) $\theta = 0.7$(MS=1.7085).

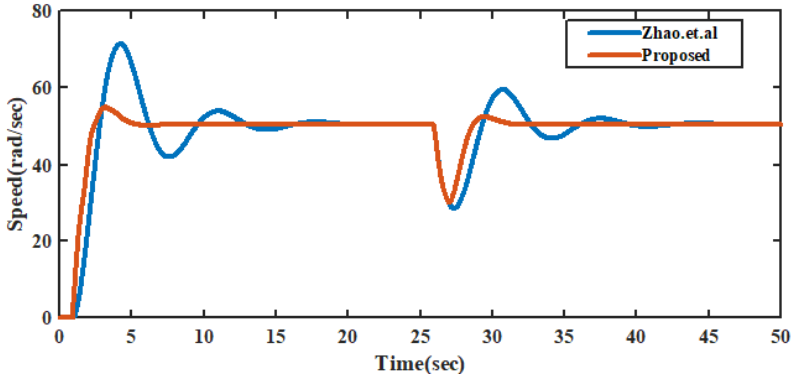

(b) $\theta = 0.9$(MS=2.032)

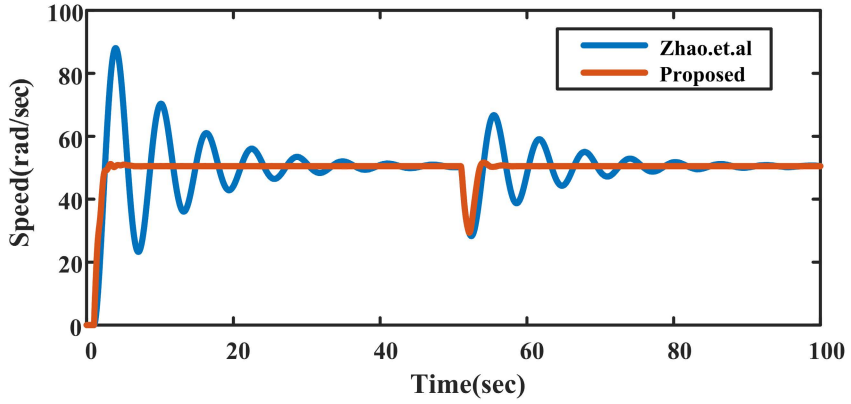

(c) $\theta = 1$(MS=3.36)

FIGURE 20. Speed response at different time delays of Quanser DC servo motor.

instances of time as presented in Equation 31. For this analysis set point is considered as 50 rad/sec

$$Disturbance(d) = \begin{cases} -0.5 \ units, & at \ t = 20 \ sec \\ 0.5 \ units, & at \ t = 40 \ sec \\ -1 \ units, & at \ t = 60 \ sec \\ 1 \ units, & at \ t = 80 \ sec \end{cases} \quad (31)$$

The disturbance rejection case response of both methods is depicted in Figure 19. From Figure 19, it is observed that the proposed method gave a superior response.

For further critical analysis, both the methods are tested for different time delays and the response is presented in Figure 20. At a particular time delay both the methods are tuned for same MS and compared. From Figure 20, it is clear that as the time delay increases, Zhao *et al.* [22] method's performance declines while the proposed method is able to perform well. Zhao *et al.* [22] method performs well for lower time delay values but as the time delay increases the performance decline relatively. Overall, the proposed method is able to deliver better performance in terms of speed and robustness when compared to the opposite method.

V. CONCLUSION

A novel control strategy is proposed for stable and unstable FOPDT.The controller parameters are derived using the polynomial method. Higher order dead time approximation and higher-order filter are employed for more accuracy which has thus resulted in improved performance characteristics. Tuning guidelines are developed predicated on the loop transfer function's maximum sensitivity. The proposed method engenders superior response characteristics than subsisting control techniques in the literature. The proposed control technique is capable of achieving efficacious control over delay-dominant processes. To address applicability to non-linear processes, the proposed method is verified for a nonlinear chemical reactor. The proposed control strategy is also tested in real-time for regulating the speed of the DC servo motor. In future work, the authors would like to extend the proposed work for stable and unstable higher-order processes with time delay and inverse response processes. Also, the authors would like to extend the present work for multi-loop control structures, fractional order filters, etc.

REFERENCES

[1] J. G. Ziegler and N. B. Nichols, "Optimum settings for automatic controllers," *Trans. ASME*, vol. 64, no. 11, pp. 1–7, 1942.
[2] A. M. De Paor, "A modified Smith predictor and controller for unstable processes with time delay," *Int. J. Control*, vol. 41, no. 4, pp. 1025–1036, 1985.
[3] H. J. Kwak, S. W. Sung, I.-B. Lee, and J. Y. Park, "A modified Smith predictor with a new structure for unstable processes," *Ind. Eng. Chem. Res.*, vol. 38, no. 2, pp. 405–411, Feb. 1999.
[4] S. Majhi and D. P. Atherton, "Obtaining controller parameters for a new Smith predictor using autotuning," *Automatica*, vol. 36, no. 11, pp. 1651–1658, 2000.
[5] X.-P. Yang, Q.-G. Wang, C. C. Hang, and C. Lin, "IMC-based control system design for unstable processes," *Ind. Eng. Chem. Res.*, vol. 41, no. 17, pp. 4288–4294, Aug. 2002.
[6] W. Tan, H. J. Marquez, and T. Chen, "IMC design for unstable processes with time delays," *J. Process Control*, vol. 13, no. 3, pp. 203–213, Apr. 2003.
[7] W. Zhang, D. Gu, W. Wang, and X. Xu, "Quantitative performance design of a modified Smith predictor for unstable processes with time delay," *Ind. Eng. Chem. Res.*, vol. 43, no. 1, pp. 56–62, Jan. 2004.
[8] T. Liu, Y. Z. Cai, D. Y. Gu, and W. D. Zhang, "New modified Smith predictor scheme for integrating and unstable processes with time delay," *IEE Proc.-Control Theory Appl.*, vol. 152, no. 2, pp. 238–246, Mar. 2005.
[9] T. Liu, W. Zhang, and D. Gu, "Analytical design of two-degree-of-freedom control scheme for open-loop unstable processes with time delay," *J. Process Control*, vol. 15, no. 5, pp. 559–572, Aug. 2005.
[10] X. Lu, Y.-S. Yang, Q.-G. Wang, and W.-X. Zheng, "A double two-degree-of-freedom control scheme for improved control of unstable delay processes," *J. Process Control*, vol. 15, no. 5, pp. 605–614, Aug. 2005.
[11] A. S. Rao and M. Chidambaram, "Enhanced Smith predictor for unstable processes with time delay," *Ind. Eng. Chem. Res.*, vol. 44, no. 22, pp. 8291–8299, Oct. 2005.
[12] W. Zhang, "Optimal design of the refined Ziegler–Nichols proportional-integral-derivative controller for stable and unstable processes with time delays," *Ind. Eng. Chem. Res.*, vol. 45, no. 4, pp. 1408–1419, 2006.
[13] A. S. Rao, V. S. R. Rao, and M. Chidambaram, "Simple analytical design of modified Smith predictor with improved performance for unstable first-order plus time delay (FOPTD) processes," *Ind. Eng. Chem. Res.*, vol. 46, no. 13, pp. 4561–4571, Jun. 2007, doi: 10.1021/ie061308n.
[14] M. Shamsuzzoha and M. Lee, "Analytical design of enhanced PID filter controller for integrating and first order unstable processes with time delay," *Chem. Eng. Sci.*, vol. 63, no. 10, pp. 2717–2731, May 2008.
[15] W. Tan, "Analysis and design of a double two-degree-of-freedom control scheme," *ISA Trans.*, vol. 49, no. 3, pp. 311–317, Jul. 2010.
[16] B. del-Muro-Cuéllar, J. F. Márquez-Rubio, M. Velasco-Villa, and J. de Jesús Álvarez-Ramírez, "On the control of unstable first order linear systems with large time lag: Observer based approach," *Eur. J. Control*, vol. 18, no. 5, pp. 439–451, Jan. 2012. [Online]. Available: https://www.sciencedirect.com/science/article/pii/S0947358012709627
[17] V. Vijayan and R. C. Panda, "Design of PID controllers in double feedback loops for SISO systems with set-point filters," *ISA Trans.*, vol. 51, no. 4, pp. 514–521, Jul. 2012.
[18] M. Ajmeri and A. Ali, "Two degree of freedom control scheme for unstable processes with small time delay," *ISA Trans.*, vol. 56, pp. 308–326, May 2015.
[19] K. G. Begum, A. S. Rao, and T. K. Radhakrishnan, "Maximum sensitivity based analytical tuning rules for PID controllers for unstable dead time processes," *Chem. Eng. Res. Des.*, vol. 109, pp. 593–606, May 2016. [Online]. Available: https://www.sciencedirect.com/science/article/pii/S0263876216300077
[20] P. K. Medarametla and M. Muthukumarasamy, "A novel PID controller with second order lead/lag filter for stable and unstable first order process with time delay," *Chem. Product Process Model.*, vol. 13, no. 1, 2018, Art. no. 20170010, doi: 10.1515/cppm-2017-0010.
[21] Q. Wang, C. Lu, and W. Pan, "IMC PID controller tuning for stable and unstable processes with time delay," *Chem. Eng. Res. Des.*, vol. 105, pp. 120–129, Jan. 2016.
[22] Z.-C. Zhao, Z.-Y. Liu, and J.-G. Zhang, "IMC-PID tuning method based on sensitivity specification for process with time-delay," *J. Central South Univ. Technol.*, vol. 18, no. 4, pp. 1153–1160, Aug. 2011.
[23] M. Irshad and A. Ali, "Robust PI-PD controller design for integrating and unstable processes," *IFAC-PapersOnLine*, vol. 53, no. 1, pp. 135–140, 2020.
[24] S. Nema and P. Kumar Padhy, "Identification and cuckoo PI-PD controller design for stable and unstable processes," *Trans. Inst. Meas. Control*, vol. 37, no. 6, pp. 708–720, Jul. 2015.
[25] K. Lu, W. Zhou, G.-Q. Zeng, and Y. Zheng, "Constrained population extremal optimization-based robust load frequency control of multi-area interconnected power system," *Int. J. Electr. Power Energy Syst.*, vol. 105, pp. 249–271, Feb. 2019.

[26] K.-D. Lu, G.-Q. Zeng, and W. Zhou, "Adaptive constrained population extremal optimisation-based robust proportional-integral-derivation frequency control method for an islanded microgrid," *IET Cyber-Syst. Robot.*, vol. 3, no. 3, pp. 210–227, 2021.
[27] G. Lloyds Raja and A. Ali, "New PI-PD controller design strategy for industrial unstable and integrating processes with dead time and inverse response," *J. Control, Autom. Electr. Syst.*, vol. 32, no. 2, pp. 266–280, Apr. 2021.
[28] C.-T. Liou and C. Yu-Shu, "The effect of nonideal mixing on input multiplicity in a CSTR," *Chem. Eng. Sci.*, vol. 46, no. 8, pp. 2113–2116, 1991.

KURUNA DIVAKAR received the B.Tech. degree in electrical and electronics engineering from JNTUH, Andhra Pradesh, India, and the M.Tech. degree in power electronics from JNTUA, Andhra pradesh. He is currently pursuing the Ph.D. degree with the Control and Automation Department, Vellore Institute of Technology, Vellore, India. His research interests include process dynamic control and system theory.

M. PRAVEEN KUMAR received the B.E. degree in electronics and instrumentation engineering from Andhra University, Visakhapatnam, India, the M.Tech. degree in instrumentation and control systems from the Jawaharlal Nehru Technological Institute (JNTU), Kakinada, India, and the Ph.D. degree in control system engineering from the Vellore Institute of Technology (VIT) University, Vellore, Tamil Nadu, India. He has authored over 20 research papers in journals and conferences. He is currently an Assistant Professor (sr) with the School of Electrical Engineering, VIT University. His interests include process control and virtual instrumentation.